International Journal of Mass Spectrometry 300 (2011) 59–64

Contents lists available at ScienceDirect

International Journal of Mass Spectrometry

journal homepage: www.elsevier.com/locate/ijms

Quantitative mass spectrometry by orthogonal projection method with periodic signal of electrostatic ion beam trap

Qi Sun[a,*], Changxin Gu[a], Li Ding[b]

[a] Department of Materials Science, Fudan University, 220 Handan Rd., Shanghai, 200433, People's Republic of China
[b] Shimadzu Research Laboratory Shanghai Co. Ltd., 108 Second Kayuan Rd, Shanghai 201201, People's Republic of China

ARTICLE INFO

Article history:
Received 29 September 2010
Received in revised form
13 December 2010
Accepted 14 December 2010
Available online 22 December 2010

Keywords:
Orthogonal projection method (OPM)
Quantitative mass spectrometry
Electrostatic ion beam trap (EIBT)
Orthogonal projection mass spectrometry
(OPMS)

ABSTRACT

In this paper, orthogonal projection method (OPM) is introduced which could perform quantitative mass spectrometry with signal of electrostatic ion beam trap (EIBT). In order to acquire periodic current signal, a model of EIBT with cylindrical-detector is set up to simulate ions oscillatory motion. Where after, OPM is introduced and applied for quantitative mass spectrometry. It shows that quantitative MS with high precision could be obtained by OPM with sampling time short as 200 μs. Comparing with FFT, the mass spectrometry performed by OPM is characterized by higher precision and much shortened sampling time. OPM mass spectrometry is influenced by several factors, including the length of sampling time, mass detecting interval δM, tested ion mass and its location in the mass detecting interval, which are discussed systematically. The OPM results show that, the effective sampling time for quantitative MS should be prolonged when the tested ion mass is increased or the mass detecting interval is decreased. The shortest effective sampling time T_{90S} and the longest effective sampling time T_{90L} are all proportional to $M^{3/2}/\delta M$, and the relation of which is specified by linear regression.

1. Introduction

EIBT (electrostatic ion beam trap) has been invented and developed during the last decade, which stores and manipulates ions with only electrostatic fields [1–4]. When a group of ions is injected into EIBT, they would be trapped and oscillate between the two parallel sets of electrode mirrors with applied voltages, which working principle is similar to that of an optical resonator, and accordingly endows EIBT with another name of ion-trap resonator [5–7]. It has been demonstrated that EIBT is a competent instrument to perform various experiments both in physics and in chemistry, such as lifetime measurement of metastable state atomic, molecular and negative ions [8–11], electron-impact experiments [12,13], beam dynamics and mass spectrometry [14,15].

As the ions are constrained by the electrode mirrors, they oscillate back and forth and induce periodic current signal on the detector which is mounted in the middle of EIBT [16]. The periodicity of the signal characterizes the mass of the oscillating ions, and with frequency analysis of which, the mass spectrometry can be performed. Consequently, EIBT could be used as time-of-flight mass spectrometry, in which the flight path of the ions is multiple folded by electrode mirrors, and thus high resolution of mass analysis is expected.

FFT (fast Fourier transform) is conventional method to analyse periodic signal and acquire frequency spectrum, and the EIBT mass spectrometry acquired are all based on this method [14,15]. However, the frequency spectrum of FFT is quite complex, in addition to the fundamental harmonic, more than ten higher order harmonics exist with prominent intensity, which encumbers mass spectrometry, especially different kinds of ions compounded together. In addition, more accurate frequency spectrum means longer sampling time, and which should be at least several hundreds milliseconds to perform MS. In the case of prolonged sampling time, the dispersion effect of the ions should be taken into consideration, which would tamper the periodicity of the oscillating ions and do harm to mass spectrometry. Moreover, it is impossible to indicate the quantity of the detected ions through frequency analysis of FFT.

In this paper, orthogonal projection method (OPM) is introduced which could perform quantitative mass spectrometry with high precision and with much shortened sampling time. Current signals of ions with certain mass number are adopted as basis vectors in OPM, which is consistent with particular EIBT setup. The current signal of tested ions could be orthogonal projected to these basis vectors, and the coefficients of projection could not only specify the mass number of the tested ions, but also indicate the amount of those ions. As shown in this paper, sampling time of OPM is much shortened comparing with FFT, e.g., for ions with mass number ~100, quantitative MS above 90% accuracy can be acquired with sampling time short as several

---

* Corresponding author. Tel.: +86 21 65643649; fax: +86 21 65643647.
E-mail address: sqhit@fudan.edu.cn (Q. Sun).

1387-3806/$ – see front matter © 2010 Elsevier B.V. All rights reserved.
doi:10.1016/j.ijms.2010.12.010

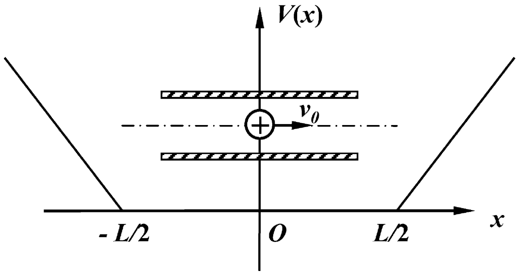

Fig. 1. Schematic figure of linear trapping potential field of EIBT with single-cylindrical detector mounted in the middle.

hundreds microseconds, which is impossible to be performed by FFT.

The model that generates EIBT periodic signal is described in Section 2, and orthogonal projection method is introduced in Section 3. Results and discussion are presented in Section 4, in which several factors that influence the result of OPM mass spectrometry are discussed, and conclusions are given in Section 5.

2. Numerical modeling

In order to simulate the motion of the ions and acquire the periodic signal, a model of EIBT is established. According to the experimental setup [14], the whole length of EIBT is set to be 400 mm, and the length of central field-free region is set to be 200 mm. A linear trapping potential field that constrains ions motion is set up in EIBT as shown in Fig. 1, and the electric field is formulated as a function of $\boldsymbol{x}$.

$$E(x)=\begin{cases} k & x<-L/2 \\ 0 & |x|<L/2 \\ -k & x>L/2 \end{cases} \tag{1}$$

where L corresponds to the length of central field-free region, and the gradient k of potential characterizes the electric field in the region of electrostatic mirrors. In the central field-free region of EIBT, a single-cylinder detector is used to detect the induced current, and the details of the modeling of induced current have been discussed in the former publication [16,17]. The length and radius of the cylindrical detector are selected to be 10 mm and 5 mm respectively.

Moving ion with mass m is assumed to carry single charge e, with its initial position being set in the center of the potential field as shown in Fig. 1. The initial velocity v_0 is determined by the initial energy E_0 according to Eq. (2)

$$v_0=\sqrt{\frac{2E_0}{m}} \tag{2}$$

In the simulation, E_0 is set to be 4.2 keV and k is set to be 200 kV/m, and thus the oscillation period of argon ions in such an modeling setup is about 6 μs.

In order to simplify the problem, following assumptions are introduced:

1. Moving ions are assumed to have the same energy with neglecting their energy dispersion.
2. The ions move along the axis of the cylindrical detector, and their energy remains unchanged when passing through the detector. This assumption is legitimate as discussed previously [16,17].
3. As sampling time in the simulation is restricted in 10 ms, Coulomb reaction between positive charged ions is not considered in the simulation.

According to the assumptions above, the only force seen by the moving ions is the electric force applied by the electrodes. The ions motion equation is

$$E(x)e=m\frac{d^2x}{dt^2} \tag{3}$$

Leap-frog differential scheme is applied to acquire ions velocity and ions position at each time step. With the simulation results of the ions motion, the periodic image current signal induced on the detector could be acquired, which corresponds to the ions oscillate with certain frequency according to their mass [14,15].

According to the idealized simulation setup, the period T_0 of the ion with mass m and charge e is

$$T_0=\left(\frac{2L}{\sqrt{2E_0}}+\frac{4\sqrt{2E_0}}{ke}\right)\sqrt{m} \tag{4}$$

With introducing specified E_0, k, L and relative constants, the period of ions motion in this model EIBT is

$$T_0=0.630168\sqrt{M}\,(\mu\text{s}) \tag{5}$$

Where M is the mass number of the moving ions. As single-cylindrical detector is adopted in the simulation to detect image current signal, the period of the signal is one half of that of the ions motion

$$T_s=\frac{T_0}{2}=0.315084\sqrt{M}\,(\mu\text{s}) \tag{6}$$

And the frequency of the detected signal is

$$f_s=\frac{3.173757}{\sqrt{M(\text{amu})}}\,(\text{MHz}) \tag{7}$$

and the mass number M is related to the signal frequency according to

$$M=\frac{10.07273}{f_s^2} \tag{8}$$

As the period of signal acquired in EIBT is proportional to the square root of the ions mass number, and with determining the frequency of the signal by frequency analysis (e.g., FFT), the mass number of the ions can be specified by Eq. (8).

In Fourier transform, the length of sampling time T in time domain determines Δf, the indeterminacy in frequency domain, which satisfies the relation of $\Delta f = 1/T$. And the relation between the indeterminacy of mass number and that of frequency is derived from Eqs. (7) and (8)

$$\Delta M=0.630168M^{3/2}\Delta f \tag{9}$$

Accordingly, the longer sample time implies the higher precision of frequency analysis. In our simulation, the length of longest sampling time is selected to be 10 ms, thus $\Delta f = 0.0001$ MHz, and according to Eq. (9), the indeterminacy of mass number is

$$\Delta M=6.30168\times10^{-5}M^{3/2} \tag{10}$$

From the equation it is clearly shown that, ΔM increases with increasing the mass number with the order of 1.5, which means the indeterminacy of mass increases remarkably with increasing the mass of the detected ions.

Fig. 2(a) shows the periodic image current signal induced by the ions of mass number 100.01 with 10 ms sampling time and 10 ns sampling interval, and the ions' number is selected to be unit amount. Fig. 2(b) is the corresponding frequency spectrum performed by FFT. As shown in the figure, the signal waveform deviates evidently from the harmonic waves, which are used as the basis function in FT, and thus brings complexity to FFT frequency spectrum. In addition to the fundamental harmonic which corresponds

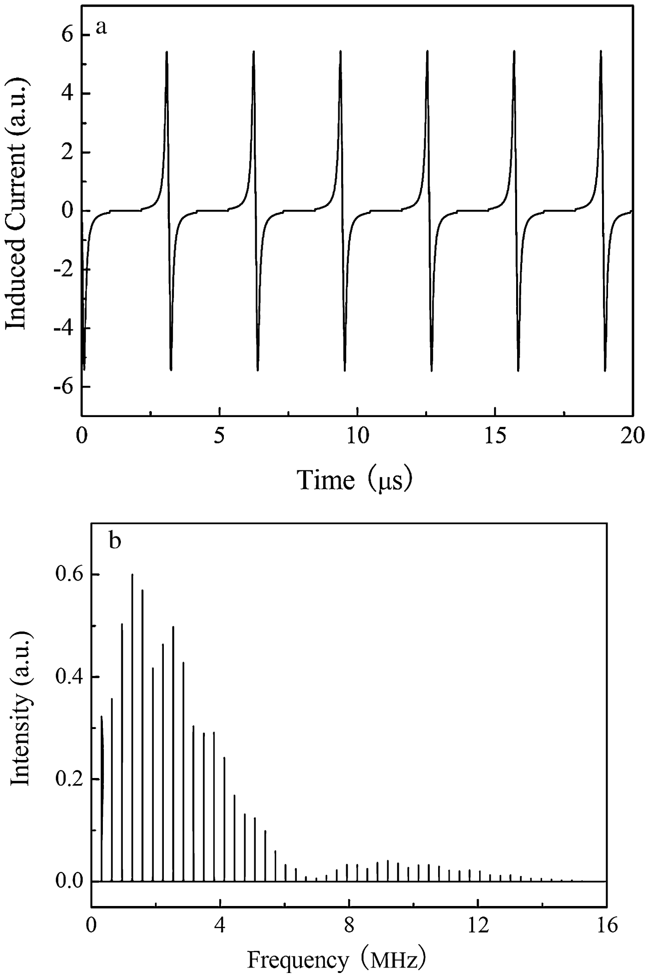

Fig. 2. (a) Periodic image current signal induced by the ions of mass number 100.01 with 10 ms sampling time and 10 ns sampling interval; (b) corresponding frequency spectrum by FFT.

to the frequency of the signal, the frequency spectrum consists of many higher order harmonics, and it is the 4th harmonic frequency that possesses the highest intensity. With specifying the fundamental frequency, $f_s = 0.31738$ MHz, the mass number determined is 99.997 with indeterminacy ± 0.063, and the resolving power of mass spectrometry is about 1600.

The complexity of the frequency spectrum encumbers mass spectrometry, especially different kinds of ions compounded together, and decreases the efficiency of the usage of the signal. Furthermore, it is impossible to perform quantitative mass spectrometry through such frequency analysis.

3. Orthogonal projection method (OPM)

According to functional analysis, the signal of EIBT belongs to space $L^2(R)$, that is, Lebesgue square integrable space, and FFT realizes least square approximation to the original signal by taking harmonics as basis vectors [18]. The mathematical concept of OPM proposed in this study is identical to that of FFT, which also projects detected current signal to a linear vector space spanned by basis vectors, while OPM adopts induced signals of EIBT themselves as basis vectors, not harmonics in FFT. As discussed in this paper, this method could perform quantitative mass spectrometry with high precision. Comparing with FFT, the mass spectrometry acquired by OPM is characterized by a more readable spectrum, a much shortened sampling time and the ability to do quantitative analysis.

Apparently, the induced current signals corresponds to different mass numbers are linear independent, that is, any signal cannot be linearly expressed by any other signals of different mass numbers. As the signal of certain mass number is taken as the basis vector, a set of such basis vectors of different mass numbers spans an inner product space, and for any signal that is projected into this space, its orthogonal projection could be expressed by the linear combination of these basis vectors. The coefficients of orthogonal projection characterize the composition of the signal, and thus the mass analysis is performed.

The current signal induced by the oscillating ions with certain ion mass and unit amount is taken as a basis vector, and a set of such current signals constructs a set of basis vectors, which are linear independent and span into a vector space V

$$\text{The basis vectors :} \quad \{x_1, x_2, \ldots, x_m\}$$

$$\text{And the vector space } V: \; V = span\{x_1, x_2, \ldots, x_m\}$$

The vector $\mathbf{x_i} = (x_{i1}, x_{i2}, \ldots, x_{iN})^T \in R^N$, is the element in N-tuple space, where N is the sample number of vector $\mathbf{x_i}$, and the standard inner product is defined

$$\left\langle \mathbf{x_i}, \mathbf{x_j} \right\rangle = \sum_{k=1}^{N} x_{ik} \cdot x_{jk} \tag{11}$$

and norm is also defined as

$$\|\mathbf{x_i}\| = \sqrt{\langle \mathbf{x_i}, \mathbf{x_i} \rangle} \tag{12}$$

This set of basis vectors is not orthonormal basis, because the norm of the basis vectors are not unity, that is, $\|\mathbf{x_i}\| \neq 1$; and although the vectors are independent they are not orthogonal to each other, that is, $\left\langle \mathbf{x_i}, \mathbf{x_j} \right\rangle \neq 0, (i \neq j)$.

The current signal of the tested ions is considered as vector $\mathbf{v}$, which is also an element in N-tuple space but does not belong to space V spanned by the basis vectors, that is, $\mathbf{v} = (v_1, v_2, \ldots, v_N)^T \in R^N$ and $\mathbf{v} \notin V$. The orthogonal projection of $\mathbf{v}$ in space V is $\mathbf{v}_0$, which could be uniquely expressed by the linear combination of basis vectors as the basis vectors are linear independent,

$$\mathbf{v}_0 = \sum_{j=1}^{m} \alpha_j \mathbf{x}_j \tag{13}$$

According to the property of orthogonal projection [19], $\mathbf{v}_0$ is closest to $\mathbf{v}$ among all vectors in space V, that is

$$\|\mathbf{v} - \mathbf{v}_0\| = \min_{w \in V} \|\mathbf{v} - \mathbf{w}\| \tag{14}$$

Thus the vector $\mathbf{v} - \mathbf{v}_0$ is orthogonal to space V, which means it is orthogonal to any vector in space V, including each basis vector $\mathbf{x_i}$.

$$\left\langle \mathbf{v} - \mathbf{v}_0, \mathbf{x}_i \right\rangle = 0 \quad (i = 1, \ldots, m) \tag{15}$$

And thus

$$\left\langle \mathbf{v}_0, \mathbf{x}_i \right\rangle = \left\langle \mathbf{v}, \mathbf{x}_i \right\rangle \tag{16}$$

Combining with Eq. (13), Eq. (16) becomes

$$\left\langle \sum_{j=1}^{m} \alpha_j \mathbf{x}_j, \mathbf{x}_i \right\rangle = \left\langle \mathbf{v}, \mathbf{x}_i \right\rangle \tag{17}$$

For certain basis vector $\mathbf{x}_i$, an equation with m unknown α_j is established

$$\sum_{j=1}^{m} \left(\sum_{k=1}^{N} x_{jk} \cdot x_{ik} \right) \alpha_j = \sum_{k=1}^{N} v_k \cdot x_{ik} \tag{18}$$

For i from 1 to m, a set of linear equations with m unknown α_j is constructed, and α_j could be acquired by solving these equations. As coefficients α_js specify the weights of the signal with unknown mass number projected to each basis vector, the quantitative mass spectrometry can be performed by analysing these coefficients of projection.

The basis vectors of the induced signal can be generated by simulation as well as by experiment, the latter of which would includes the influences of practical factors. As discussed thoroughly in the previous study [16,17], the induced current signal of certain mass number on the detector could be linearly transformed to the current signal of ions with different mass number, with firstly generating a sample signal experimentally, other basis vectors could be calibrated and generated by simulation.

4. Results and discussion

A tested signal of ions with mass number 100.01 and unit amount has been generated by the model of EIBT for orthogonal projection. Mass detecting range can be determined by FFT and is set to be 90–110 with mass detecting interval $\delta M = 0.1$. Basis vectors are all generated by the same model with unit amount which correspond to the ions with mass number specified by the detecting range and interval. Sampling interval is 10 ns throughout the study, and different lengths of sampling time are adopted to study its effect on orthogonal projection mass spectrometry (OPMS).

Fig. 3 shows the results of orthogonal projection mass spectrometry with sampling time being 0.01 ms, 0.04 ms and 0.2 ms. As sampling time is short as 0.01 ms, the noise of background is rather high, but the projection coefficients is prominent for mass number 100 and 100.1, which is 0.64 and 0.34 respectively, as shown in Fig. 3(a). Such projection result is consistent with the fact that the mass number of tested ions is laid between these two mass numbers. As sampling time is increased, the precision of orthogonal projection is increased. The projection coefficient of mass number 100 is increased to 0.90 for 0.04 ms and 0.98 for 0.2 ms, while the coefficient of 100.01 is decreased to 0.16 for 0.04 ms and 0.1 for 0.2 ms, as shown in Fig. 3(b) and (c). The basis vector of mass number 100.0 has the largest weight, and the coefficient of projection is consistent with the intensity of the tested signal. It is also shown from the figure that, as the sampling time is prolonged, not only the precision of quantitative mass spectrometry is increased, but the noise of background is also suppressed.

Fig. 4 shows the results of orthogonal projection mass spectrometry with sampling time being 0.4 ms, 2 ms and 4 ms. As sampling time prolonged further, the projection coefficient of mass number 100 is decreased from 0.98 for 0.4 ms to 0.72 for 2 ms and 0.33 for 4 ms, while the coefficient of 100.01 is decreased from 0.08 for 0.4 ms to 0.005 for 2 ms and 10^{-6} for 4 ms. Comparing Figs. 3 and 4, it is clearly shown that, as sampling time is short, the difference between the basis vectors and the tested signal is not very evidently, and OPMS is obtained with low precision and high background noise. With prolonging the length of sampling time, the advantage of the basis vector that is nearest to the test signal is shown, and the coefficient is prominent for this basis vector, which position and coefficient determine the mass number and the quantity of the tested signal. As the sampling time prolonged even longer, the difference between the nearest basis vector and tested signal becomes larger which decreases the projection coefficient to this nearest vector. From Figs. 3 and 4, it can be deduced that there exists a range of effective sampling time for the tested ions with certain mass number, within which the quantitative MS with high precision can be performed. It also implies that the prolonged sampling time demands a finer detecting interval, which will reinforce the similarity between the tested signal and the basis vectors.

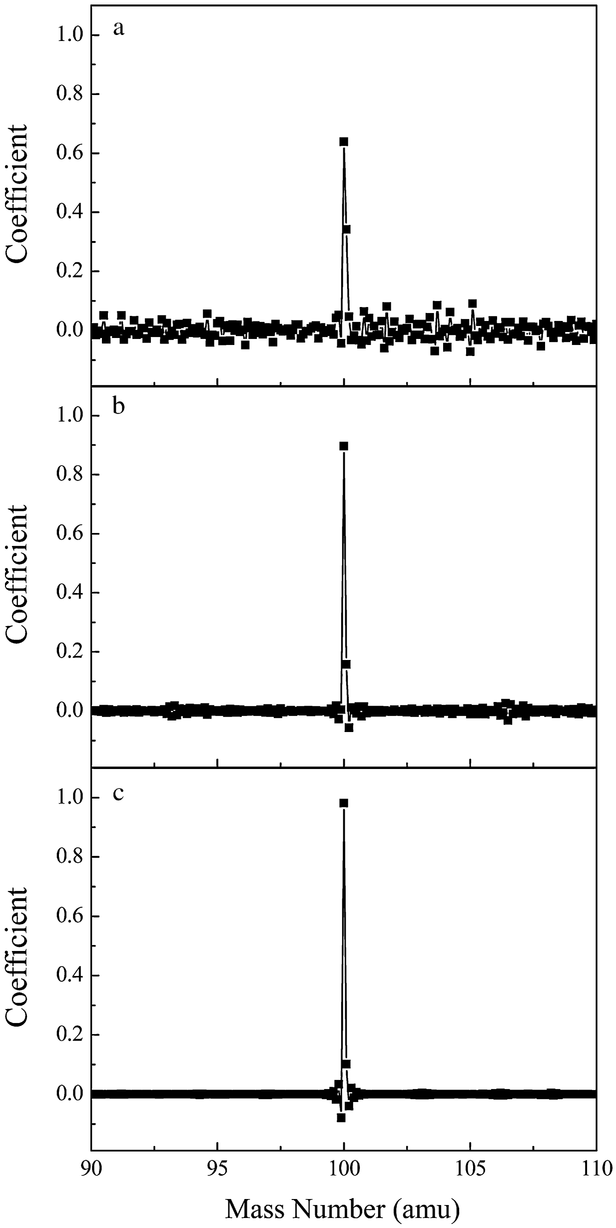

Fig. 3. Orthogonal projection mass spectrometry of ions with mass number 100.01; (a) 10 μs sampling time; (b) 40 μs sampling time; (c) 200 μs sampling time.

Fig. 5 shows the OPMS for tested signal with mass number from 100.01 to 100.09 with space 0.01, to study the influence of location of the tested mass in the mass detecting interval. Sampling time is selected to be 100 μs in which case the quantitative MS can be acquired with high precision for the tested ion with mass number 100.01. As the tested ion shifted from 100.01 to 100.09 in the detecting interval δM, the coefficient of mass number 100.0 decreases and that of 100.1 increases, both monotonously. For the tested mass 100.05 being in the middle of the interval, the coefficients of 100.0 and 100.1 are both about 0.6 and almost equal to each other. As the mass number of the tested ion is shifted nearer to the higher mass number of the interval, the coefficient of the higher mass number increases. It is shown from Fig. 5 that the selection of the basis vectors and the partition of the mass detecting range will influence the precision of OPMS, which is suggested to be overcome by scanning basis vectors, which will relocate the tested ion mass number in the proper position of the mass detecting interval.

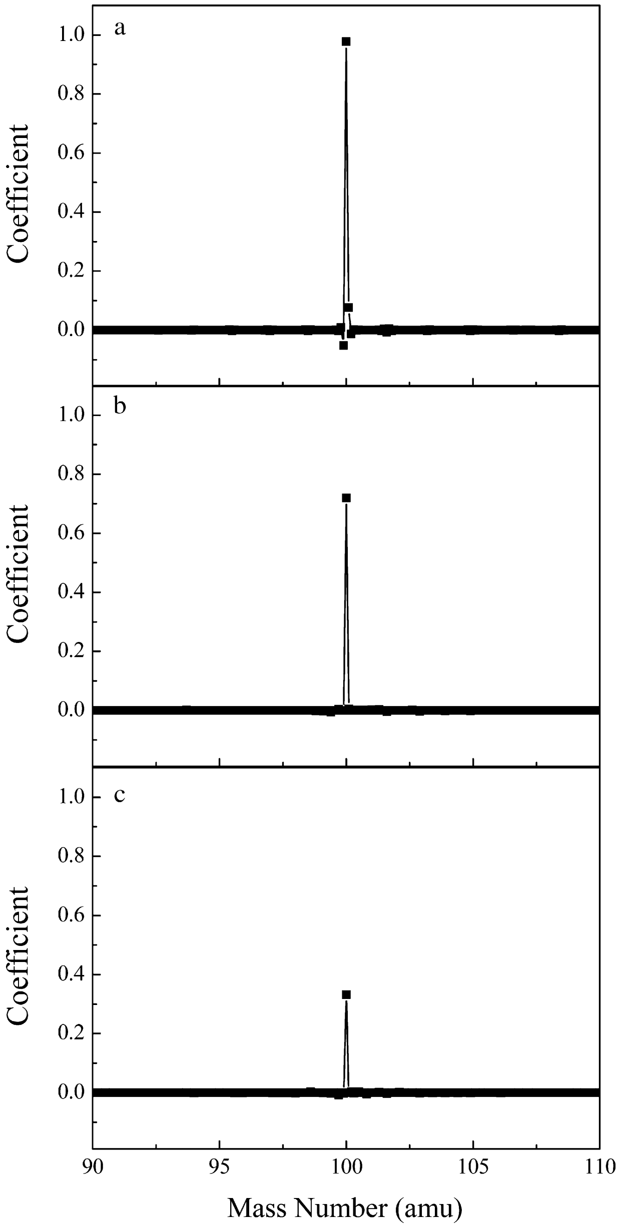

Fig. 4. Orthogonal projection mass spectrometry of ions with mass number 100.01; (a) 400 μs sampling time; (b) 2000 μs sampling time; (c) 4000 μs sampling time.

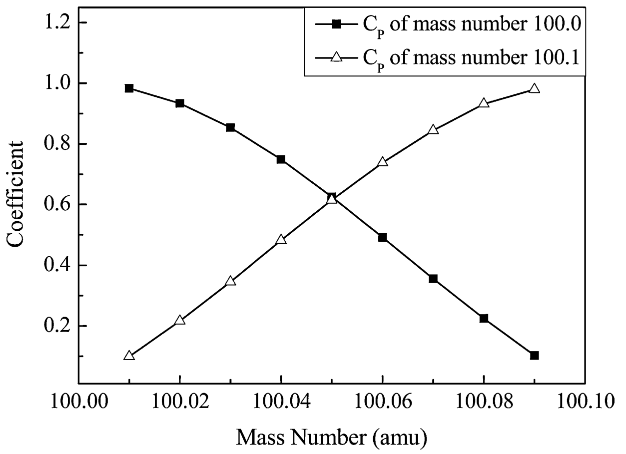

Fig. 5. Coefficients of projection of tested ions with mass number from 100.01 to 100.09 with mass space 0.01.

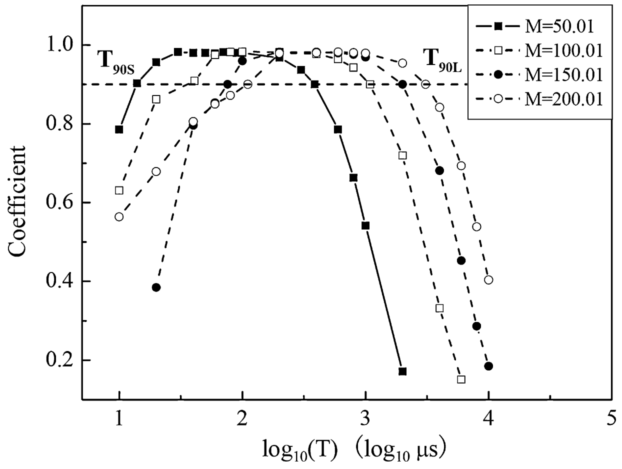

Fig. 6. Relation between the length of sampling time and the coefficient of orthogonal projection mass spectrometry.

Fig. 6 shows the relation between sampling time and the coefficient of OPM. As the sampling time spans a large time scale, the logarithm scale is adopted in the time axis. Two parameters, T_{90S} and T_{90L} are introduced, which indicate the shortest sampling time and longest sampling time that both acquire the coefficient of 0.9 respectively. With such definition, the quantitative MS with 90% accuracy will be acquired in the sampling time range from T_{90S} to T_{90L}. As shown in the figure, the sampling time for ions with different mass numbers all shows the same trend, and effective sampling time range shifted to longer time end for large mass number.

It shows that effective sampling time relates with the mass number being tested, M, and the mass detecting interval δM. With increasing mass number, the sampling time to acquire high precision quantitative MS should be prolonged, while the finer mass detecting interval δM also requires prolonged sampling time. Fig. 7 shows the relation between mass detecting interval δM and the length of sampling time, which is indicated by T_{90S} and T_{90L}, and the mass number of the tested ions is 100.01. The inverse proportionality is clearly shown by the linear fit line both for T_{90S} and for T_{90L}.

The OPM results show that, the effective sampling time for quantitative MS should be prolonged when the tested ion mass is increased or the mass detecting interval is decreased. It is found by trial that T_{90S} and T_{90L} are all proportional to $M^{3/2}/\delta M$, and the relation of which can be specified by linear regression. Fig. 8 shows

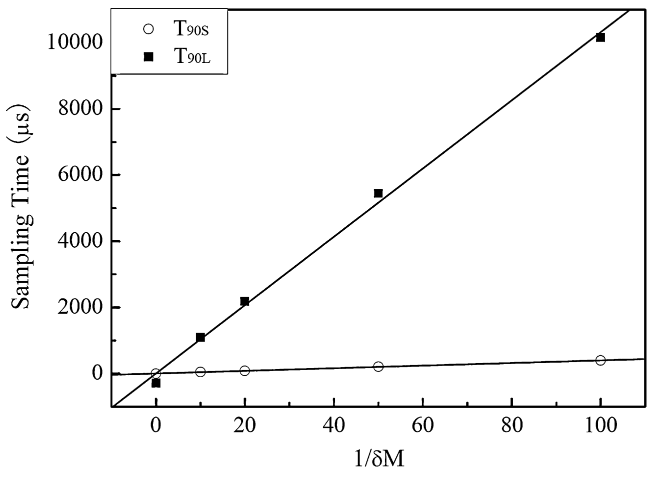

Fig. 7. Inverse proportional relation between the length of sampling time and mass detecting interval δM, with tested mass number being 100.01.

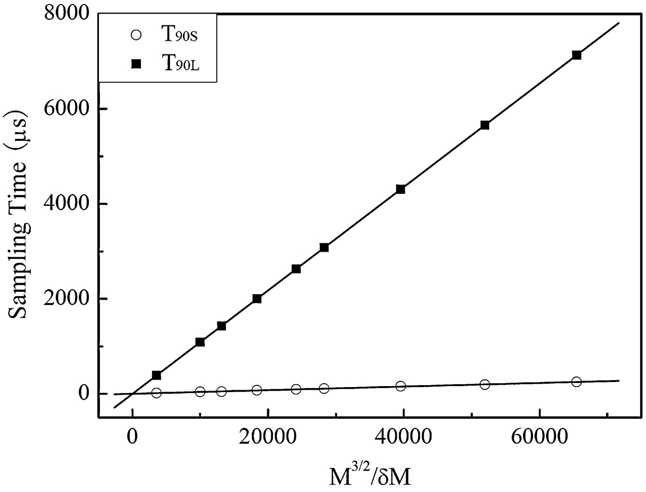

Fig. 8. Linear relation between the length of sampling time and $M^{3/2}/\delta M$.

linear relation between sampling time ($T_{90\mathrm{S}}$ and $T_{90\mathrm{L}}$) and $M^{3/2}/\delta M$, and the linear relation is characterized by two linear formulas

$$T_{90\mathrm{S}} = \frac{2.63167 + 0.0377M^{3/2}}{\delta M}\,(\mu\mathrm{s}) \tag{19}$$

And

$$T_{90\mathrm{L}} = \frac{0.21941 + 0.1089M^{3/2}}{\delta M}\,(\mu\mathrm{s}) \tag{20}$$

The correlation coefficient of these two linear regressions is 0.998 and 1 respectively, and as a reasonable approximation, the shortest sampling time for 90% accuracy quantitative MS can be determined by $T_{90\mathrm{S}} = 0.0377M^{3/2}/\delta M\,(\mu\mathrm{S})$, and the longest sampling time can be determined by $T_{90\mathrm{L}} = 0.1089M^{3/2}/\delta M\,(\mu\mathrm{s})$. It should be noted that these linear coefficients are associated with particular setup of EIBT and the structure of image current detector, and are specific for present discussion. For different setups of the instrument, the linear relation between sampling time and $M^{3/2}/\delta M$ remains, while the coefficients should be determined by experiment or simulation.

5. Conclusion

In this paper, orthogonal projection method (OPM) is introduced which could perform quantitative mass spectrometry with signal of electrostatic ion beam trap (EIBT). Firstly, a model of EIBT with cylindrical-detector is set up to simulate ions oscillatory motion and generate periodic current signal. Where after, OPM is introduced and applied for quantitative mass spectrometry which adopting EIBT signal itself as basis vector. It shows that quantitative MS with high precision could be obtained by OPM with sampling time short as 200 μs. Comparing with FFT, the mass spectrometry performed by OPM is characterized by higher precision of quantitative analysis and much shortened sampling time. There exists an effective sample time range (from $T_{90\mathrm{S}}$ to $T_{90\mathrm{L}}$), within which quantitative MS could be performed with accuracy over 90%. As the detected mass number increases, the effective sampling time range shifted to longer time range; and while detecting time interval δM decreases, both $T_{90\mathrm{S}}$ and $T_{90\mathrm{L}}$ increase. It is found that $T_{90\mathrm{S}}$ and $T_{90\mathrm{L}}$ are all proportional to $M^{3/2}/\delta M$, and the relation of which is specified by linear regression, which could be used to instruct the selection of proper sampling time and mass detecting interval of OPMS.

References

[1] D. Attia, D. Strasser, O. Heber, M.L. Rappaport, D. Zajfman, Nucl. Instrum. Meth. A 547 (2005) 279.
[2] M. Dahan, R. Fishman, O. Heber, M.L. Rappaport, N. Altstein, D. Zajfman, W.J. van der Zande, Rev. Sci. Instrum. 69 (1998) 76.
[3] D. Zajfman, D. Strasser, O. Heber, S. Goldberg, A. Diner, M.L. Rappaport, Nucl. Instrum. Meth. A 532 (2004) 196.
[4] T. Suzuki, Y. Yamauchi, Nucl. Instrum. Meth. A 562 (2006) 53.
[5] H.B. Pedersen, D. Strasser, B. Amarant, O. Heber, M.L. Rappaport, D. Zajfman, Phys. Rev. A 65 (2002) 042704.
[6] H.B. Pedersen, D. Strasser, O. Heber, M.L. Rappaport, D. Zajfman, Phys. Rev. A 65 (2002) 042704.
[7] H.B. Pedersen, D. Strasser, S. Ring, O. Heber, M.L. Rappaport, Y. Rudich, I. Sagi, D. Zajfman, Phys. Rev. Lett. 87 (2001) 055001.
[8] A. Wolf, K.G. Bhushan, I. Ben-Itzhak, N. Altstein, D. Zajfman, O. Heber, M.L. Rappaport, Phys. Rev. A 59 (1999) 267.
[9] L. Knoll, K.G. Bhushan, N. Altstein, D. Zajfman, O. Heber, M.L. Rappaport, Phys. Rev. A 60 (1999) 1710.
[10] K.G. Bhushan, H.B. Pedersen, N. Altstein, O. Heber, M.L. Rappaport, D. Zajfman, Phys. Rev. A 62 (2000) 012504.
[11] O. Heber, R. Golser, H. Gnaser, D. Berkovits, Y. Toker, M. Eritt, M.L. Rappaport, D. Zajfman, Phys. Rev. A 73 (2006) 060501 (R).
[12] O. Heber, P.D. Witte, A. Diner, K.G. Bhushan, D. Strasser, Y. Toker, M.L. Rappaport, I. Ben-Itzhak, N. Altstein, D. Schwalm, A. Wolf, D. Zajfman, Rev. Sci. Instr. 76 (2005) 013104.
[13] L.H. Andersen, O. Heber, D. Zajfman, J. Phys. B: Atom. Mol. Opt. Phys. 37 (2004) R57.
[14] D. Zajfman, Y. Rudich, I. Sagi, D. Strasser, D.W. Savin, S. Goldberg, M.L. Rappaport, O. Heber, Int. J. Mass Spectrom. 229 (2003) 55.
[15] K.G. Bhushan, S.C. Gadkari, J.V. Yakhmi, V.C. Sahni, Rev. Sci. Instrum. 78 (2007) 083302.
[16] Q. Sun, C.X. Gu, L. Ding, Nucl. Instr. Meth. Phys. Res. A 609 (2009) 177.
[17] Q. Sun, C.X. Gu, L. Ding, Int. J. Mass Spectrom. 282 (2009) 38.
[18] A. Boggess, F.J. Narcowich, A First Course in Wavelets with Fourier Analysis, Publishing House of Electronics Industry, Beijing, 2004.
[19] K. Hoffman, R. Kunze, Linear Algebra, Prentice Hall, Upper Saddle River, NJ, 2008.